Universality of DNA Adsorption Behavior on the Cationic Membranes of Nanolipoplexes

Giulio Caracciolo,*,† Daniela Pozzi,† Augusto Amici,‡ and Heinz Amenitsch§

Department of Chemistry, 'Sapienza' University of Rome, P.le Aldo Moro 5, 00185, Rome, Italy, Department of Molecular Cellular and Animal Biology, University of Camerino, Via Gentile III da Varano, 62032 Camerino (MC), Italy, and Institute of Biophysics and Nanosystems Research, Austrian Academy of Sciences, Schmiedelstrasse 6, A-8042 Graz, Austria

Received: October 29, 2009; Revised Manuscript Received: December 21, 2009

Nanolipoplexes have emerged worldwide as the most prevalent synthetic gene delivery system. Nowadays, it is accepted that complete DNA protection and a precise control of the physical attributes of emerging complexes are major steps toward rational design of efficient nanocarriers. Here we revise the mechanism of DNA adsorption to the cationic membranes of lipid nanovectors. Here we show that both the DNA-binding ability of cationic membranes and the one-dimensional DNA packing density inside the complex depend on the cationic lipid/anionic DNA charge ratio. Remarkably, both these distributions are rescaled on universal curves when plotted against γ, a dimensionless quantity expressing the ratio between the area of cationic membranes and that occupied by DNA molecules. As a result, the DNA condensation on the surface of lipid nanocarriers can be regarded as a two-step process. Our findings indicate a successful way to the rational design of next-generation drug delivery nanocarriers.

Introduction

In the coming decades, nanomedicine is believed to offer hope with some of the most intractable disease classes using nanomaterials that, due to their small size, are able to gain access to, and operate within, the cell.[1−3] Cancers, inherited diseases, cardiovascular diseases, and many others are targets for this novel medical approach. Among potential gene nanocarriers, cationic liposomes (CLs) made of cationic and zwitterionic lipids have emerged worldwide as the most prevalent synthetic carriers.[4,5] CLs, when mixed with DNA, spontaneously form stable complexes (lipoplexes) that can deliver DNA into cells by binding electrostatically to their anionic membranes. In these self-assembled complexes, the cationic lipid head groups neutralize the phosphate groups on the DNA chains, effectively releasing the counterions previously bound electrostatically to lipids and DNA, thus gaining translational entropy.[6−10] Recent high-resolution synchrotron small-angle X-ray scattering (SAXS) studies[11−16] have shown that the most abundant phase is a multilamellar structure (L_α^C phase, Figure 1) with DNA monolayers sandwiched between cationic membranes.

To date, a rational approach for the design of optimal lipoplex formulations has been severely limited by a poor understanding of the physical attributes of cationic membranes regulating the equilibrium structure of lipoplexes. Such an urgent requirement motivated us to investigate the condensation behavior of DNA on cationic membranes. Focusing on the transfection-relevant excess cation lipid regime,[13] the main question addressed here is which are the physical principles regulating the DNA binding by CLs. This point is recognized as an essential step toward the development of highly efficient gene delivery systems.

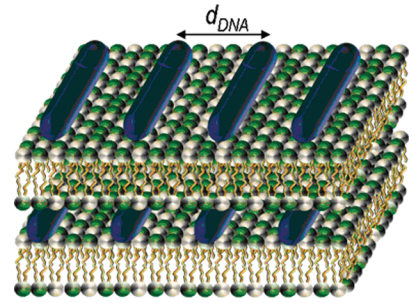

Figure 1. Schematics of the lamellar phase of lipoplexes. DNA rods (blue) are sandwiched between cationic membranes made of cationic (green) and neutral (white) lipids.

To this end, we used electrophoresis on agarose gels to determine the DNA-binding ability of CLs. This experimental technique was chosen because it provides very precise determination of free DNA that is not protected by lipids.[15] High-resolution synchrotron SAXS was used for determination of the nanostructure of lipoplexes.

Here, we show that lipoplexes containing excess cationic charge coexist with unbound plasmid DNA indicating that the phase diagram of lipoplexes is more complex than previously considered.[6−8,13] According to previous findings,[13] the one-dimensional (1D) DNA packing density, as determined by synchrotron SAXS experiments, exhibited large variations between different liposome formulations. Crucially, we show that, irrespective of liposome formulations and cationic lipid/DNA charge ratio, both DNA-binding ability of CLs and DNA packing density are rescaled on universal curves when the interfacial area of lipid membranes is considered. Moreover, we have also clarified the role of electrostatic interactions on the DNA packing density within lamellar complexes. This is fundamental since rational design of next-generation lipid nanovectors requires a coherent understanding of their structures and interactions.

* To whom correspondence should be addressed. Address: Chemistry Department, University of Rome "La Sapienza", Piazzale A. Moro n. 5, 00185 Rome, Italy. Phone: (+39)06-49913076. Fax: (+39)06-490631. E-mail: g.caracciolo@caspur.it.

† 'Sapienza' University of Rome.

‡ University of Camerino.

§ Austrian Academy of Sciences.

10.1021/jp9103382
Published on Web 01/15/2010

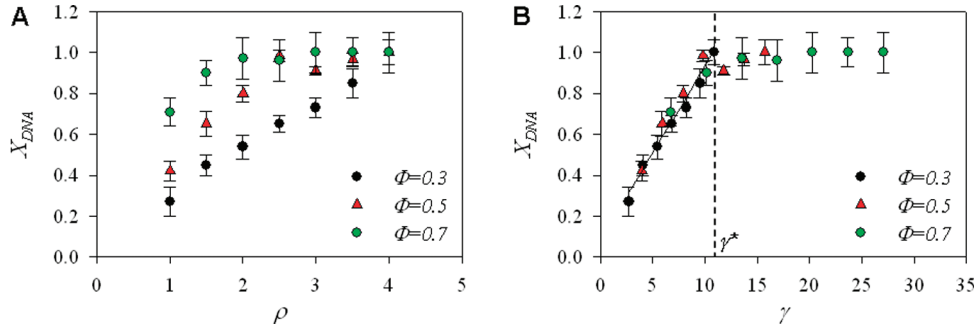

Figure 2. DNA-binding ability of cationic liposomes with different neutral/total lipid molar fraction, Φ, as a function of the cationic/anionic charge ratio, ρ. Panel A: molar fraction of plasmid DNA protected by cationic liposomes, X_{DNA}, as a function of the cationic lipid/DNA charge ratio, ρ. Panel B: molar fraction of plasmid DNA protected by CLs, X_{DNA}, as a function of γ. Rescaled distribution shows a linear increase with γ. Solid line is the best linear fit to the data. Dashed line indicates the γ value (γ^*) for which complete DNA protection occurs.

Experimental Section

Liposome and Lipoplex Preparation. Cationic lipid 1,2-dioleoyl-3-trimethylammonium-propane (DOTAP) and zwitterionic lipid dioleoylphosphocholine (DOPC) were purchased from Avanti Polar Lipids (Alabaster, AL) and used without further purification. DOTAP-DOPC CLs were prepared following standard protocols[17] at a molar ratio of neutral lipid in the bilayer of $\Phi = L_0/(L_C + L_0) = 0.3$, 0.5, and 0.7, where L_0 and L_C are moles of neutral and cationic lipids, respectively. The final concentration of lipid solutions was 1 mg/mL for both SAXS and electrophoresis experiments. By sonication, small unilamellar vesicles (SUV) with narrow particle size distributions (diameter, $d = 100 \pm 5$ nm; pdi = 0.2; data not shown) were prepared. Mixing adequate amounts of the DNA solutions with suitable volumes of liposome dispersions resulted in the spontaneous formation of self-assembled DOTAP-DOPC/DNA complexes. Lipoplexes were prepared with several cationic lipid/DNA ratios (mol/mol) (i.e., ρ = (cationic lipid (by mole)/DNA base) = 0.5, 1, 1.5, 2, 2.5, 3, 3.5, 4, 4.5, 5).

Estimation of Molar Fraction of DNA Protected by Cationic Lipids. Electrophoresis studies were conducted on 1% agarose gels containing Tris-borate-EDTA (TBE) buffer. Lipoplexes were prepared by mixing adequate amounts of lipid dispersions (1 mg/mL, Tris-HCl buffer) with 6.75 μg of pGL3 control plasmid. After electrophoresis, ethidium bromide (Et-Br) was added. The electrophoresis gel was observed and digitally photographed using a Kodak Image Station (model 2000 R, Kodak, Rochester, NY). Digital photographs were elucidated using dedicated software (Kodak MI, Kodak) that allows us to calculate the molar fraction of released DNA, X_{DNA}.

Determination of Lipoplex Nanostructure. SAXS measurements were carried out at the ID2 high-brilliance beamline at the European Synchrotron Radiation Facility (Grenoble, France). The energy of the incident beam was 12.5 KeV ($\lambda = 0.995$ Å); the beam size was 100 μm; and the sample-to-detector distance was 1.2 m. The diffraction patterns were collected with a 2D CCD detector (Frelon Camera). A q range from $q_{min} = 0.04$ Å^{-1} to $q_{max} = 0.5$ Å^{-1} with a resolution of 5×10^{-4} Å^{-1} (fwhm) was used. The sample was held in a 1 mm glass capillary (Hildberg, Germany). Measurements were performed at 25 °C. To avoid radiation damage, a maximum exposure time of 3 s/frame was used for any given sample. Satisfactory statistics were obtained by repeating several measurements on fresh samples. The collected 2D powder diffraction spectra were angularly integrated as elsewhere described.[18] These data were then corrected for the detector efficiency, empty sample holder, and bulk solution.

Results and Discussion

In this study, we first examined the role of membrane charge density of cationic membranes on the DNA-binding ability of CLs. CLs made of the cationic lipid 1,2-dioleoyl-3-trimethylammonium-propane (DOTAP) and zwitterionic lipid dioleoylphosphocholine (DOPC) were used. These lipids were chosen because they are widely used for transfection studies both in vitro and in vivo. CLs with different membrane charge density were prepared by changing the molar fraction of neutral lipid in the bilayer, $\Phi = L_0/(L_C + L_0)$ (L_0 and L_C indicate the moles of neutral and cationic lipid, respectively). Such an approach provides an example of controlled systematic variations of surface properties of CLs that could affect the DNA condensation behavior.

In Figure 2 (panel A), we report the molar fraction of plasmid DNA protected by lipids, X_{DNA}, as a function of the cationic lipid/DNA charge ratio, ρ, for three formulations with different membrane charge densities ($\Phi = 0.3$, 0.5, 0.7). The transfection relevant excess cationic charge regime ($\rho > 1$) was chosen because lipoplexes must be positive to bind electrostatically to mammalian cells, which contain surface proteoglycans with negatively charged sulfated groups. At the isoelectric point ($\rho = 1$), X_{DNA} was found to be lower than 1 for all lipoplex formulations. Since assuming the coexistence of unprotected plasmid DNA with DNA-free unilamellar liposomes is not realistic at all,[6−8] this finding clearly indicates that lipoplexes containing excess cationic charge coexisted with unbound plasmid DNA. According to recent findings,[17] the most compelling explanation is that there are not enough lipids to complex all the DNA. The latter observation is noteworthy especially in view of previous studies[9,10,13] that claimed that: (i) stoichiometrically charge-neutral lipoplexes ($\rho = 1$) are one-phase systems with all the DNA and the lipids associated within the complex; (ii) lipoplexes prepared above the isoelectric point ($\rho > 1$) can be only found in coexistence with CLs. Aside from understanding the exact phase diagram of lipoplexes, significant implications arise for transfection experiments where protection of DNA by cationic lipids is an essential requisite for efficient transfection. Indeed, free plasmid DNA is easily digested by DNA-ase the cytoplasm is rich in and can not reach the nucleus where transcription occurs. We therefore underline that this should be kept in mind in designing complexes for cell transfection properly, since simple count of the nominal charge ratio may be patently misleading to assess whether a lipoplex formulation can protect the DNA efficiently or not. For $\rho > 1$, phase coexistence of cationic DOTAP-DOPC/DNA lipoplexes with free DNA spanned over a relatively large range of charge ratios

whose extension decreased with increasing Φ. The latter observation means that, fixing the cationic lipid/DNA charge ratio (i.e., fixing ρ) and enriching the cationic membranes with neutral lipid (i.e., increasing Φ), complexation of larger amounts of DNA occurs.

A first step toward taking into account variations in DNA-binding ability between different liposome formulations is to recognize that at fixed ρ complexes with higher Φ have larger lipid surface area. It is natural then to try to factor out the bias induced by the difference in Φ by considering a relative indicator, that is, a dimensionless quantity expressing the ratio between the area of cationic membranes, A_L, and that occupied by DNA molecules, A_D

$$\gamma = \frac{A_L}{A_D} = \rho \frac{\left(a_C + a_0 \frac{\Phi}{1-\Phi}\right)}{2R_D l_D} \quad (1)$$

where $a_C = 62$ Å^2 and $a_0 = 72$ Å^2 denote the cross-sectional area per cationic DOTAP and neutral DOPC[19] (the removal of DOPC phosphate resulting in DOTAP justifies the lower value of a_C with respect to a_0); R_D is the radius of DNA molecules plus a hydration shell; and l_D is the mean distance between two adjacent negative charges projected on the DNA axis $l_D = 1.7$ Å.[6−8] This is a very natural choice since, upon formation of lipoplexes, cationic lipid surface becomes the site of a two-dimensional (2D) adsorption of DNA chains.[6−8,20] Figure 2 (panel B) shows that plotting X_{DNA} versus γ leads to a very good collapse of all curves for different values of Φ onto a single shape demonstrating that γ is a key parameter for 2D DNA condensation on cationic lipid membranes. The distribution then seems to be universal for all formulations considered. Interestingly, the universal curve is fitted by a linear behavior $X_{DNA} = \alpha\gamma$ (with $\alpha = 0.092$) and saturates for $\gamma > \gamma^* \sim 11$ (Figure 2, panel B, dashed line). The value of correlation coefficient ($R = 0.975$) indicates that a linear fit to the data is good. The physical meaning of Figure 2 (panel B) seems to be that the DNA-binding ability of cationic liposomes is a linear function of interfacial area of lipid membranes. Above the transition point ($\gamma > \gamma^*$), we observe that plasmid DNA is completely protected by cationic lipids independently from the cationic to anionic charge ratio, ρ, and the molar fraction of neutral lipid in the bilayer, Φ. As a consequence, complexes with very different membrane charge density (Φ) and charge ratio (ρ) but with similar lipid surface area are expected to exhibit the very same DNA binding capacity. We emphasize that the primary outcome of such a novel data interpretation is that the spatial dimension available plays a key role in the DNA-binding ability of lipoplexes.[20−23] Since the complete DNA protection is absolutely needed for efficient transfection, while the use of an excess amount of cationic lipid is detrimental in terms of toxicity to the cells, our results seem to contain a strategy for transfection studies: employing those lipoplex formulations that guarantee full DNA protection with the lowest amount of cationic lipid.

Over the past decade, synchrotron SAXS has been used to elucidate the structure of lipoplexes at the angstrom scale. As previously described, the DNA intercalated between cationic membranes forms a one-dimensional array of chains which uniformly cover the available lipid area with an average DNA interhelical distance d_{DNA} ranging from approximately 25 Å, where the DNA rods are nearly touching, to about 60 Å.[13] Variation of DNA packing density with ρ and Φ has already been investigated.[11−16,22,23] However, our novel findings about the correlation between interfacial area of CLs and their DNA-binding ability motivated us to revise the interpretation of 1D DNA packing density within lamellar lipoplexes. We therefore collected synchrotron SAXS patterns of a series of DOTAP-DOPC/DNA complexes as a function of ρ and Φ. Figure 3 (panel A) shows representative synchrotron SAXS patterns of DOTAP-DOPC/DNA complexes with $\Phi = 0.5$ as a function of ρ. Two sets of Bragg peaks were distinguished. The sharp peaks labeled q_{00n} arise from the lamellar periodicity along the normal to lipid bilayer, d, which is the sum of the membrane thickness, d_B, and the thickness of the water/DNA layer, d_W: $d = d_B + d_W = 2\pi/q_{001}$ (Figure 1). The diffuse broad peak (marked by an arrow) results from 1D ordering of the DNA sandwiched between the lipid bilayers.[4−7] It is usually referred to as "DNA peak" and corresponds to a DNA interhelical spacing $d_{DNA}=2\pi/q_{DNA}$ (Figure 1). While the position of the lamellar peaks is almost insensitive to ρ, the DNA peak shifts to smaller q with increasing ρ. From this figure, it is clear that increased ρ forces the DNA molecules to move apart. Figure 3 (panel B) shows the SAXS patterns of DOTAP-DOPC/DNA lipoplexes with the same charge ratio ($\rho = 1$) as a function of Φ. We observe that, at fixed ρ, an increase in Φ produces the monotonous dilution of the DNA lattice, i.e., the enlargement in the DNA interdistances.

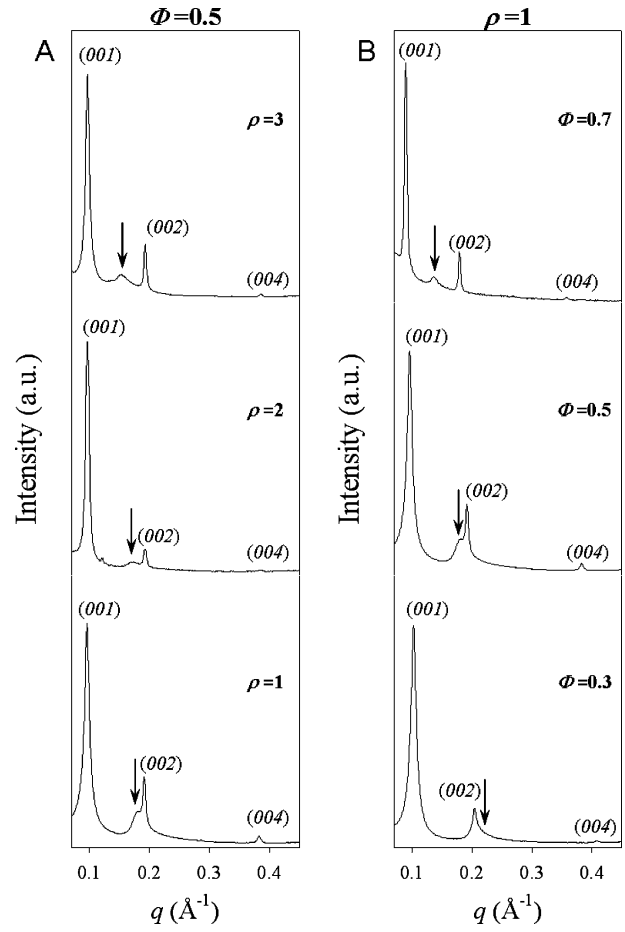

Figure 3. SAXS patterns of lipoplexes as a function of the cationic/anionic charge ratio, ρ, and the neutral/total lipid molar fraction, Φ. Panel A: SAXS patterns of DOTAP-DOPC/DNA lipoplexes at $\Phi = 0.5$ as a function of ρ. The diffuse broader peak (marked by an arrow) resulted from one-dimensional ordering of the DNA sandwiched between the lipid bilayers. Panel B: SAXS patterns of isoelectric DOTAP-DOPC/DNA lipoplexes ($\rho = 1$) as a function of the neutral/total lipid molar fraction Φ. The DNA peak is marked by an arrow.

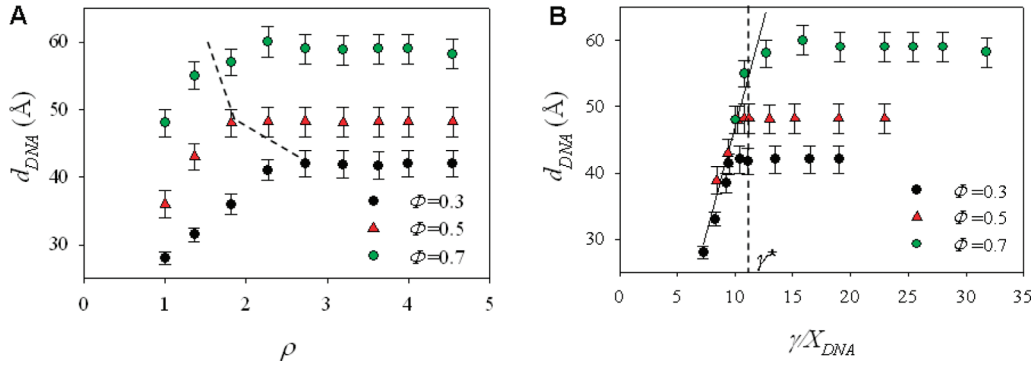

Figure 4. Interhelical DNA−DNA distance within lipoplexes with different neutral/total lipid molar fraction, Φ, as a function of the cationic/anionic charge ratio, ρ. Panel A: $d_{DNA}(\rho)$ curves for DOTAP-DOPC/DNA lipoplexes with different Φ. Dashed lines are a guide to the eye that links ρ saturation values. Panel B: when plotting d_{DNA} against γ, all the data points coalescence onto a single curve. Solid line is the best fit to the data using eq 2. Dashed line is the lowest γ value (γ^*) for which d_{DNA} plateaus.

We show in Figure 4 (panel A) a set of d_{DNA} curves for DOTAP-DOPC/DNA lipoplexes with different Φ as a function of ρ. All the profiles exhibit a common behavior: the interhelical spacing, d_{DNA}, increases linearly with ρ and saturates for $\rho = \rho^*$. On the other side, we observe that increasing membrane charge density (i.e., decreasing Φ) results in: (i) a marked decrease of the linear slope and (ii) a significant increase in the saturation point values (Figure 4, panel A, dashed line). While the former observation has already been explained,[6−10,13] the latter remains under debate. Previous investigations[8,9,13] suggested that the uptake of excess lipid into the complex continues above the isoelectric point[13] as long as the interbilayer repulsions become sufficiently large to forbid further accommodation of bilayer into the complex. Despite its good soundness, a simple electrostatic interpretation has some shortcomings, as already pointed out by some authors.[17,21−23] Indeed, if the intake of excess lipid is stopped by the electrostatic interaction between excess cationic bilayers, such repulsions are expected to be higher at lower Φ (i.e., at higher membrane charge density).[21−24] As a result, saturation values are expected to decrease with decreasing Φ. As evident, these concepts are in disagreement with experimental findings of Figures 2 and 4 (panel A) showing that complexes with lower Φ continue absorbing excess cationic lipid and remain one phase for higher ρ than those with higher Φ. Thus, the problem of 2D DNA condensation, as considered to date, apparently runs into a puzzle. However, the universal scaling on DNA condensation reported in Figure 2 (panel B) provides a solid grounding for comparison between packing of DNA rods in lipoplex formulations with different values of Φ and ρ. To make this visually evident, we have plotted the DNA−DNA interdistance against γ. Figure 4 (panel B) shows that the large variability of DNA packing density, as observed in Figure 4 (panel A), is rescaled away if d_{DNA} is plotted versus γ/X_{DNA}. Remarkably, in rescaling the 1D DNA packing density by γ/X_{DNA}, a universal linear increase of d_{DNA} is found, independent of Φ and ρ. This finding is most likely to mean that the interhelical DNA−DNA distance is mainly regulated by the interfacial area of lipid membranes that is available to 2D DNA condensation. Remarkably, after rescaling, we observe that adsorption of excess lipid is inversely proportional to Φ with saturation values now appearing to be in reverse order (Figure 4, panel B, dashed line) with respect to when d_{DNA} is plotted against the cationic lipid/DNA charge ratio, ρ (Figure 4, panel A, dashed line). Finally, this result is consistent with the physical expectation that complex affinity for excess cationic lipid is inversely proportional to membrane charge density of lipid membranes.

To make observations quantitative, we also calculated the average DNA−DNA interdistance within lamellar lipoplexes. DNA molecules projected onto cationic membranes can be regarded as parallel ribbons of width $D = 25$ Å.[8,9,16] Ribbons are supposed to occupy homogeneously all of the available area of cationic lipid membranes that are treated as flat planes of uniform membrane charge density.[8,9] By simple geometric considerations, the average DNA−DNA interdistance comes to be

$$d_{DNA} = \frac{D}{4X_{DNA}}\gamma \qquad (2)$$

Equation 2 relies on the basic assumption that all lipid and plasmid DNA protected by lipids, X_{DNA}, are associated within the complex. This assumption seems most logical because coexistence of pure cationic liposomes and unbound DNA, if any, should occur in very limited regions of the phase diagram.[6−8] Interestingly, the universal scaling curve of Figure 4 (panel B) is fitted reasonably well by eq 2 when experimental values of X_{DNA}, as determined by electrophoresis, are used. In our calculation D can be regarded as a fitting parameter. The value of D calculated from the linear fit to the data ($D \sim 25.6$ Å) is in excellent agreement with the diameter of DNA molecules plus a thin hydration shell ($D \sim 25$ Å).

In Figure 2 (panel B), we found γ^* as the saturation point of DNA binding, i.e., the minimum value of γ that assures complete DNA protection by lipids. For $\gamma > \gamma^*$, complexes guaranteed maximum DNA load and were therefore identical in their DNA-binding ability. On the other side, SAXS data reported in Figure 4 (panel B) show that DNA adsorption continues for $\gamma > \gamma^*$ up to d_{DNA} plateaus. The lowest saturation value ($\Phi = 0.3$) is just a bit larger than γ^* ($\gamma \sim 11.5$) suggesting that, when DNA is completely protected, strong interbilayer repulsions do not allow further lipid to accommodate. Complexes with lower membrane charge density can accommodate larger amounts of excess lipid with the result that DNA rods move apart. As a result, d_{DNA} continues to increase linearly with γ. Finally, electrostatic repulsions set an upper limit on the amount of lipid the complex can accommodate, and a specific saturation level depending on Φ is reached.

On the whole, the 2D condensation behavior can be regarded as a two-step process. In the first step ($\gamma < \gamma^*$), DNA is not completely protected by lipids, and the spacing between DNA chains is set by the geometrical constraint of the interfacial area of lipid membranes available to DNA condensation and not as

a result of a balance of attractive and repulsive forces. For $\gamma > \gamma^*$, the repulsive interaction dependent on the membrane charge density of lipid membranes is the constraint that sets the DNA packing density. It is noteworthy that our analysis identified the interfacial area of lipid membranes as a universal parameter regulating DNA condensation behavior in lamellar cationic liposome/DNA complexes. The results of our analysis are in very good agreement with previous findings indicating that the equilibrium structure of lipoplexes can strongly be influenced by size effect and packing constraints.[10,11] We may speculate that there would be practical applications of the ideas discussed in this article. For instance, one important result is that the differences in DNA-binding ability between lipoplex formulations are wide. The implications for transfection purposes could be significant. A common approach in transfection studies is characterizing lipoplex formulations with a number of variations in physical−chemical properties. This approach is suitable for analyzing data sets in search of structures of correlations. Toward a rational explanation of distinct transfection efficiencies, protection of DNA by cationic lipids must be correctly evaluated before trying to establish a correlation between the physical−chemical attributes of nanovectors and their biological activity. Finally, and perhaps most importantly, our findings may provide new tools toward an understanding of the lipoplex formation mechanism. As a key step in this direction, the universality of the observed behavior opens the door to new routes of controlling biological self-assembly for use in nanomedicine.

Conclusions

As interest in understanding the principles governing interactions between biological systems on the nanoscale grows, we expect the quest for the comprehension of transfection mechanisms to accelerate. In this article, we have presented strong evidence that the widely scattered distributions of both molar fraction of DNA protected by cationic lipids and DNA−DNA spacings within lamellar lipoplexes are rescaled on universal curves when the γ factor is used. The identification of γ as the correct metrics to compare DNA condensation in different liposome formulations suggests its use in taking properly into account the varying DNA-binding ability of CLs. It remains to be seen whether the universal condensation behavior demonstrated in this work also occurs in more complex lipoplex formulations such as those functionalized with DNA condensing polymers, fusogenic peptides, and blood proteins promoting lipoplex−cell interaction. To go beyond and to extend our conclusions to in vivo applications, understanding to what extent the DNA condensation behavior is affected by the adsorbed "protein corona"[25−27] that is associated with the nanovectors in vivo is absolutely needed. Future work will be performed in this direction.

Acknowledgment. Dr. T. Narayanan and Dr. E. Di Cola of the experimental staff of ID02 at ESRF (Grenoble, France) are gratefully acknowledged. G.C. and D.P. are indebted to Prof. R. Caminiti for supporting research.

References and Notes

(1) Lundqvist, M.; Stigler, J.; Elia, G.; Lynch, I.; Cedervall, T.; Dawson, K. A. *Proc. Natl. Acad. Sci. U.S.A.* **2008**, *105*, 14265.
(2) Gewin, V. *Nature* **2009**, *460*, 540.
(3) Nel, A. E.; Mädler, L.; Velegol, D.; Xia, T.; Hoek, E. M. V.; Somasundaran, P.; Klaessig, F.; Castranova, V.; Thompson, M. *Nat. Mater.* **2009**, *8*, 543.
(4) Felgner, P. L.; Ringold, G. M. *Nature* **1989**, *331*, 461.
(5) Tros de Ilarduya, C.; Arangoa, M. A.; Moreno-Aliaga, M. J.; Düzgüneş, N. *Biochim. Biophys. Acta* **2002**, *1561*, 209.
(6) Harries, D.; May, S.; Gelbart, W. M.; Ben-Shaul, A *Biophys. J.* **1998**, *75*, 159.
(7) May, S.; Harries, D.; Ben-Shaul, A *Biophys. J.* **2000**, *78*, 1681.
(8) May, S.; Ben-Shaul, A. *Curr. Med. Chem.* **2004**, *11*, 1241.
(9) Bruinsma, R.; Mashl, J. *Europhys. Lett.* **1998**, *41*, 165.
(10) Bruinsma, R. *Eur. Phys. J. B* **1998**, *4*, 75.
(11) Salditt, T.; Koltover, I.; Rädler, J. O.; Safinya, C. R. *Phys. Rev. Lett.* **1997**, *79*, 2582.
(12) Koltover, I.; Salditt, T.; Rädler, J. O.; Safinya, C. R. *Science* **1998**, *281*, 78.
(13) Koltover, I.; Salditt, T.; Safinya, C. R. *Biophys. J.* **1999**, *77*, 915.
(14) Caracciolo, G.; Pozzi, D.; Caminiti, R.; Congiu Castellano, A. *Eur. Phys. J. E* **2003**, *10*, 331.
(15) Wang, L.; Koynova, R.; Parikh, H.; MacDonald, R. C. *Biophys. J.* **2006**, *91*, 3692.
(16) Caracciolo, G.; Pozzi, D.; Caminiti, R.; Mancini, G.; Luciani, P.; Amenitsch, H. *J. Am. Chem. Soc.* **2007**, *129*, 10092.
(17) Henriques, A. M.; Madeira, C.; Fevereiro, M.; Prazeresa, D. M. F.; Aires-Barrosa, M. R.; Monteiro, G. A. *Int. J. Pharm.* **2009**, *377*, 92.
(18) Boesecke, P. *J. Appl. Crystallogr.* **2007**, *40*, 423.
(19) Tristram-Nagle, S.; Petrache, H.; Nagle, J. F. *Biophys. J.* **1998**, *75*, 917.
(20) Koltover, I.; Wagner, K.; Safinya, C. R. *Proc. Natl. Acad. Sci. U.S.A.* **2000**, *97*, 14046.
(21) Gonçalves, E.; Debs, R. J.; Heath, T. D. *Biophys. J.* **2004**, *86*, 1554.
(22) Caracciolo, G.; Pozzi, D.; Caminiti, R.; Amenitsch, H. *Chem. Phys. Lett.* **2006**, *429*, 250.
(23) Caracciolo, G.; Pozzi, D.; Caminiti, R. *Appl. Phys. Lett.* **2006**, *89*, 043901.
(24) Farago, O.; Grønbech-Jensen, N.; Pincus, P. *Phys. Rev. Lett.* **2006**, *96*, 018102.
(25) Cedervall, T.; Lynch, I.; Foy, M.; Berggård, T.; Donnelly, S. C.; Cagney, G.; Linse, S.; Dawson, K. A. *Angew. Chem., Int. Ed.* **2007**, *46*, 5754.
(26) Cedervall, T.; Lynch, I.; Lindman, S.; Berggård, T.; Thulin, E.; Nilsson, H.; Dawson, K. A.; Linse, S. *Proc. Natl. Acad. Sci. U.S.A.* **2007**, *104*, 2050.
(27) Lynch, I.; Cedervall, T.; Lundqvist, M.; Cabaleiro-Lago, C.; Linse, S.; Dawson, K. A. *Adv. Colloid Interface Sci.* **2007**, *134−135*, 167.

JP9103382